Proceedings of the 2014 IEEE/SICE International Symposium on System Integration, Chuo University, Tokyo, Japan, December 13-15, 2014

Biped Locomotion Control for Uneven Terrain with Narrow Support Region

Mitsuharu Morisawa, Nobuyuki Kita, Shin'ichiro Nakaoka,
Kenji Kaneko, Shuuji Kajita and Fumio Kanehiro

***Abstract*— This paper presents a biped locomotion control method for an exploration in unknown environment. It is still hard for humanoid robot to walk autonomously even an artificial construction such as a power plant which are overly arranged many stairs and pipes. In such an environment, the physical constraints with a collision avoidance, joint limitations and support region on the terrain, become dominant limitations for an exploration. Updating environmental information to biped walking pattern generator and controller, a biped walking on a complicated rough terrain can be achieved. The proposed method is validated through several dynamics simulations with the HRP-2 humanoid robot.**

I. Introduction

The advancement of robotics technologies such as environmental measurement and recognition, motion planning and control, improves a robot's autonomy. Humanoid robot is attractive platform that can be integrated by these technologies. Humanoid robots are expected to take over human's work in hazardous situations as a result of the integration. DARPA Robotics Challenge(DRC) trials in December 2013 demonstrated that humanoid robots have a potential to contribute a disaster response. The one of the greatest hurdle is their mobile ability, which is still poorer than humans. To improve an autonomy of the robot, these measurement of environment, motion planning and motion control should be executed as faster as possible.

Because of no fixed position on environment and a higher position of the center of mass, humanoid robot has to pay attention to a balance maintenance. There are various studies that have addressed this issue. Nishiwaki et al. [2] applied a preview control for online walking pattern generator to play the role of a long term stabilizer. Choi et al. [3] presented a stability proof by using the Lyapunov method for a balance control. Wieber [4] proposed the integration scheme of the COG motion with an adaptive footstep using Model Predictive Control under the linear inequality constraints. Sugihara [5] evaluated the stable pole of an inverted pendulum which maximizes the stable standing region using a method similar to the CP. Kajita et al. [6] proposed tracking control of a linear inverted pendulum for stabilization of a biped walking which balance controller is based on a state feedback of the COG and the ZMP considering a ZMP delay.

Pratt et al. [7] presented the *Capture Point* (CP) which leads a motion of the COG (Center of Gravity) to a complete stop. Takenaka et al. [8] had also focused on a divergent component which is equivalent to the CP of an inverted pendulum dynamics. A landing position is modified to prevent losing a balance according to a divergent component as a result of the *model ZMP control* which accelerates the upper body. Englsberger et al. [9] introduced two approaches for Capture Point control as balance control and extended to 3D motion[10].

M.Morisawa, N.Kita, S.Nakaoka, K. Kaneko, S.Kajita and F.Kanehiro are with Research Institute of Intelligent Systems, National Institute of Advanced Industrial Science and Technology (AIST), 1-1-1, Umezono, Tsukuba, Ibaraki, 305-8568, Japan. m.morisawa@aist.go.jp

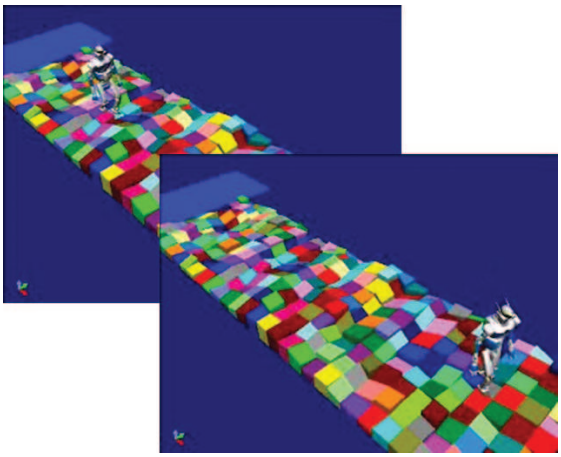

Fig. 1. Explore complicated terrain

This paper focuses on a biped locomotion control to improve a walking capability using the information of a support region as like in Fig.1. Updating a support region to the online walking pattern and a balance control will be explained in Sec.II and III-B. From a long-term point of view for a stable walking, a biped locomotion with a larger offset is easier to fall down. Thus, the CP integration is introduced to solve this problem. We proposed a new balance controler and will be formulated as PID controller in Sec.III-B. Let us explain the landing state estimation algorithm briefly to obtain a landing position and orientation, and a support region in Sec.IV. The validity of the proposed balance controller is evaluated through the simulations with several complicated environments in Sec.V.

II. Online Walking Pattern Generation

A. COG trajectory generation

A online walking pattern has been generated using an inverted pendulum model as the COG dynamics in terms of a computation cost. The inverted pendulum model with a point mass and a constant height is represented as a

978-1-4799-6944-9/14/$31.00 ©2014 IEEE

second order linear differential equation. The characteristics of this equation is known as a non-minimum phase system. Therefore, when a landing position or a landing time is changed, the ZMP trajectory is invoked an overshoot or an undershoot to accelerate or decelerate the COG. The generated ZMP has to be satisfied within a support polygon for a stable walking.

In [11], the COG trajectory is resolved to an ideal trajectory $\boldsymbol{f}$, and a tracking term $\boldsymbol{g}$.

$$\boldsymbol{x}(t_k) = \boldsymbol{f}(\boldsymbol{s}(t_k), \boldsymbol{T}(t_k), t_k) + \boldsymbol{g}(t_k) \tag{1}$$

Where, t_k denotes a current time. $\boldsymbol{s}(t_k)$ and $\boldsymbol{T}(t_k)$ are set of the desired landing position and the desired landing time which are set at t_k. When these gait parameters are changed, a discontinuity of the ideal trajectory $\boldsymbol{f}$ is occured. The tracking term $\boldsymbol{g}$ compensates these discontinuous states of the COG and the ZMP.

The ideal COG can be analyticaly derived using the piecewise polynomials of the ZMP according to the desired foot placements [11]. The tracking term generates so that the current states of the COG position x and velocity $\dot{x}$, and the ZMP position p can converge to the ideal states by a state feedback controller. A descrete-time state equation can be expressed as follow.

$$\bar{\boldsymbol{x}}_k = \begin{bmatrix} c & \frac{s}{\omega} & 1-c \\ \omega s & c & -\omega s \\ 0 & 0 & 0 \end{bmatrix} \bar{\boldsymbol{x}}_{k-1} + \begin{bmatrix} 0 \\ 0 \\ 1 \end{bmatrix} \bar{p}_k, \tag{2}$$

$$\bar{p}_k = -[k_1 \ k_2 \ k_3]\bar{\boldsymbol{x}}_{k-1}, \tag{3}$$

$$\bar{\boldsymbol{x}}_k \equiv \begin{bmatrix} \bar{x}_k & \dot{\bar{x}}_k & \bar{p}_k \end{bmatrix}^T,$$

$$c \equiv \cosh(\omega T), s \equiv \sinh(\omega T),$$

Where ω denotes a natural frequency of the inverted pendulum and T is a descrete time. Updating the COG and the ZMP by the difference from the previous and the current ideal states, the continuity of the COG and the ZMP trajectories can be guaranteed for any modification of the gait parameters. The COG trajectory can be computed robustly even if a gait parameter is changed at the end of the single support phase compared with the analytical solution [15].

$$\bar{\boldsymbol{x}}_{k-1} \leftarrow \bar{\boldsymbol{x}}_{k-1} + \boldsymbol{f}(\boldsymbol{s}(t_k), \boldsymbol{T}(t_k), t_{k-1}) - \boldsymbol{f}(\boldsymbol{s}(t_{k-1}), \boldsymbol{T}(t_{k-1}), t_{k-1}), \tag{4}$$

Notes that the feedback gains should be designed so that one of the poles is allocated to the natural frequency of an inverted pendulum[5]. This makes the stable region largely in the phase plane of the COG. The current height of the inverted pendulum is available practically for up or down waist motion as like for climbing stairs.

B. Support region constraint

As mentioned before, the ZMP is fluctuated when a gait parameter is changed during walking. The ZMP fluctuation has to be limited within the support region. Although the support region is defined spatially, this constraint of the ZMP has to be fetched in each axis independently by time varying function for the online pattern generator such as the preview controller [14]. In this paper, the support region is used as a saturate function. The support region is defined as a convex hull passed through a vertical position of the desired ZMP. Thus, the support region is not needed to represent as a time function. The future passing points of the ZMP are allocated to the center of the given support region.

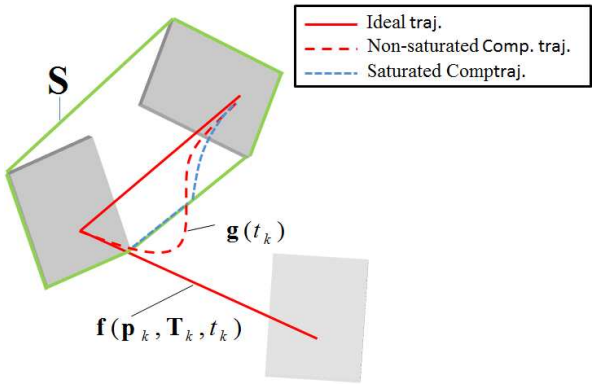

Fig. 2. ZMP trajectory within a suppport region

The ideal, the saturated and the non-saturated ZMP trajectories are illustrated in Fig.2. At first, the ideal ZMP from the desired landing position is calculated (red solid line). The red dashed line is drawn as the ZMP trajectory without a saturation according to a gait parameter modification. The saturated ZMP trajectory is shown as the blue dashed line. The spatially saturated ZMP is selected as the nearest position of the convex hull as the support region.

If the tracking term $\boldsymbol{g}$ in (1) satisfies

$$\left\{(x - p_x) + \frac{\dot{x}}{\omega}, (y - p_y) + \frac{\dot{y}}{\omega}\right\} \subset \boldsymbol{S}, \tag{5}$$

the COG and the ZMP trajectories will be stable and converge to the ideal trajectory. The equivalent condition was derived in [5].

In order to walk stably, the COG trajectory should be sequentially generated from the current status. Therefore, a current landing time is updated according to the contact phase. When a landing contact is detected at a single support phase before a preplanned landing time, the support phase is transited to a double support phase immediately.

In contrast, a landing contact is not detected until the desired landing time, a current single support period can be extended at every sampling time until the convergence condition (5) is statisfied[12]. If the COG and the ZMP states do not satisfy the stable condition, it is necessary to replan and find a feasible and a stable landing position.

III. BALANCE CONTROL

A. Inverted Pendulum Model

In order to reduce calculation costs, an inverted pendulum model has been widely used for both the COG walking motion and a balance control[2]-[14]. This paper also designs

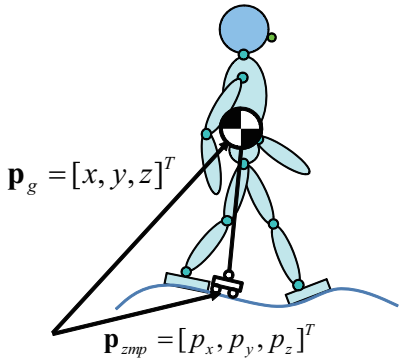

Fig. 3. Inverted Pendulum Model

a balance controller using an inverted pendulum as shown in Fig.3. To control both the COG and the ZMP, the differentiation of the ZMP $\dot{p}_x$ is set as input so that the state vector consists of the COG and the ZMP.

$$\frac{\mathrm{d}}{\mathrm{d}t}\begin{bmatrix} x \\ \dot{x} \\ p_x \end{bmatrix} = \begin{bmatrix} 0 & 1 & 0 \\ \omega^2 & 0 & -\omega^2 \\ 0 & 0 & 0 \end{bmatrix}\begin{bmatrix} x \\ \dot{x} \\ p_x \end{bmatrix} + \begin{bmatrix} 0 \\ 0 \\ 1 \end{bmatrix}\dot{p}_x, \quad (6)$$

where ω is the natural frequency of the inverted pendulum defined as

$$\omega \equiv \sqrt{\frac{g+\ddot{z}}{z-p_z}}.$$

The natural frequency ω is composed of the COG height z and gravity constant g. The height of the ZMP position p_z is traversed between the supported soles as well as the horizontal ZMP position. In this paper, the constant height of the COG is used in order to catch the control characteristics easily.

In our target humanoid robot HRP-2, elastic materials are attached below the force sensor on the ankle in order to protect against a large impact force. We assume that the ZMP dynamics can be represented as a first order delay with new ZMP input p_x^d [6]. This can be approximated as a force control characteristics of sole in more inner control loop, joint servo delay, and so on.

$$\dot{p}_x = -g_p p_x + g_p p_x^d \quad (7)$$

From (6) and (7), the system with the ZMP delay can be expressed as follows

$$\frac{\mathrm{d}}{\mathrm{d}t}\begin{bmatrix} x \\ \dot{x} \\ p_x \end{bmatrix} = \begin{bmatrix} 0 & 1 & 0 \\ \omega^2 & 0 & -\omega^2 \\ 0 & 0 & -g_p \end{bmatrix}\begin{bmatrix} x \\ \dot{x} \\ p_x \end{bmatrix} + \begin{bmatrix} 0 \\ 0 \\ g_p \end{bmatrix} p_x^d \quad (8)$$

B. Capture Point control

A design and an analysis of the Capture Point(CP) and the COG controller are shown in[9] and extended to 3D walking[10]. In previous our work[13], a balance controller with a first order delay of the ZMP for the CP was also proposed. In this paper, a balance controller with the delay model of the ZMP is performed so that the CP error can be compensated.

The Capture Point ξ_x is defined as a convergence position of the COG at infinite time.

$$\xi_x = x + \frac{\dot{x}}{\omega} \quad (9)$$

The dynamics of the inverted pendulum wiht first delay system of the ZMP can be represented by CP ξ_x and the ZMP p_x.

$$\dot{\xi}_x = \dot{x} + \frac{\ddot{x}}{\omega} = \omega(\xi_x - p_x) \quad (10)$$

From (7) and (10), the system equation can be expressed as:

$$\frac{d}{dt}\begin{bmatrix} \xi \\ \dot{\xi} \end{bmatrix} = \begin{bmatrix} 0 & 1 \\ g_p\omega & \omega - g_p \end{bmatrix}\begin{bmatrix} \xi \\ \dot{\xi} \end{bmatrix} + \begin{bmatrix} 0 \\ -g_p\omega \end{bmatrix} p^d \quad (11)$$

The system in (11) also becomes controllable. The ZMP is not included as a state variable.

Here, let us consider the following feedback controller:

$$p_x^d = -k_1\xi_x - k_2\dot{\xi}_x, \quad (12)$$

where k_1 and k_2 are the feedback gains. The relation between these feedback gains and the pole becomes

$$\begin{bmatrix} k_1 \\ k_2 \end{bmatrix} = \begin{bmatrix} -\frac{(\omega g_p + \alpha\beta)}{\omega g_p} \\ -\frac{\alpha+\beta+\omega-g_p}{\omega g_p} \end{bmatrix}. \quad (13)$$

C. Capture Point control with integration

Because of no intergration term in (12), the states error will be observed especially after walking. Therefore, (11) is added the integration term as a extended system. The target system in (11) is extended to

$$\frac{d}{dt}\begin{bmatrix} \int \xi dt \\ \xi \\ \dot{\xi} \end{bmatrix} = \begin{bmatrix} 0 & 1 & 0 \\ 0 & 0 & 1 \\ 0 & g_p\omega & \omega - g_p \end{bmatrix}\begin{bmatrix} \int \xi dt \\ \xi \\ \dot{\xi} \end{bmatrix} + \begin{bmatrix} 0 \\ 0 \\ -g_p\omega \end{bmatrix} p^d. \quad (14)$$

Let us apply a feedback controller to the error of the CP ($\xi \equiv \xi^{des} - \xi^{mes}$). Then the PID controller of the CP can be obtained corresponding to (14).

$$p^d = -k_1\int(\xi^{des} - \xi^{mes})dt - k_2(\xi^{des} - \xi^{mes}) - k_3(\dot{\xi}^{des} - \dot{\xi}^{mes}) \quad (15)$$

The CP consists of the position and the velocity of the COG defined in (9). Therefore, the CP controller in (12) and (15) contain the position, the velocity, and the acceleration of the COG. The measured value of the COG velocity and acceleration can be calculated from a pseudo derivation. The relation between the feedback gain and the pole assignment becomes:

$$\begin{bmatrix} k_1 \\ k_2 \\ k_3 \end{bmatrix} = \begin{bmatrix} -\frac{\alpha\beta\gamma}{\omega g_p} \\ -\frac{\alpha\beta+\beta\gamma+\gamma\alpha+\omega g_p}{\omega g_p} \\ -\frac{\alpha+\beta+\gamma+\omega-g_p}{\omega g_p} \end{bmatrix} \quad (16)$$

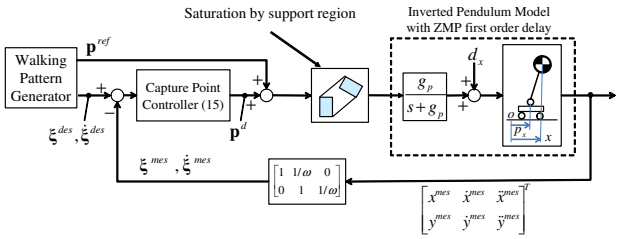

Fig. 4. Signal flow for walking control

A block diagram of the proposed balance controller is shown in Fig. 4. Summing the ZMP reference from the online walking pattern and the output of the CP controller, the ZMP command to a lower level of a force controller can be obtained. As well as the online walking pattern, the ZMP command is also saturated by the support region.

IV. Landing State Estimation

The feasible landing position and orientation of the foot can be extracted from a measured terrain information by the landing state estimation algorithm [16]. The outline of this algorithm is depicted in Fig.5. The sole of the foot is assumed to be flat and rectangular. Inputs are the position of the expected landing place (Fig.5(a)) and a point cloud around it (Fig.5(b)). An occupancy grid is set at the landing place, and occupancy probabilities of cells are calculated from the point cloud (Fig.5(c)). Convex hulls at each horizontal layer of the grid are obtained (Fig.5(d)). Based on the shape of the convex hulls, the stable poses of a foot that steps down from just above are geometrically obtained. When the desired ZMP (hereafter referred to as ZMP) is specified, the stable pose whose support region horizontally includes the ZMP is unique. Because of the quantized error or the nature of the algorithm, the obtained stable pose may not be realized. A validation process is performed against the obtained stable pose to ensure that it is firmly realized. If the validation process is passed, the obtained stable pose and its support region are output as the foot landing state. More details of this algorithm is published in [16].

V. Simulation

.

The validity of the proposed method for a biped locomotion is confirmed by a dynamics simulator implemented on Choreonoid[17]. In this simulation, we assume a square region of floor can be obtained through a stereo camera emulation. Any environment information can not be utilized directly in the online pattern generation and a balance controller. The measured floor is converted to 2cm grid map in [16]. Thus, the generated landing position and orientation include a quantization error. Therefore, the maximum position and orientation error will become ± 2[cm] and ± 8.7[deg] respectively. The robust biped locomotion control is surely needed even though in simulation.

Figure 6 shows the utilization effect of a support region during walking. When information of a support region is not

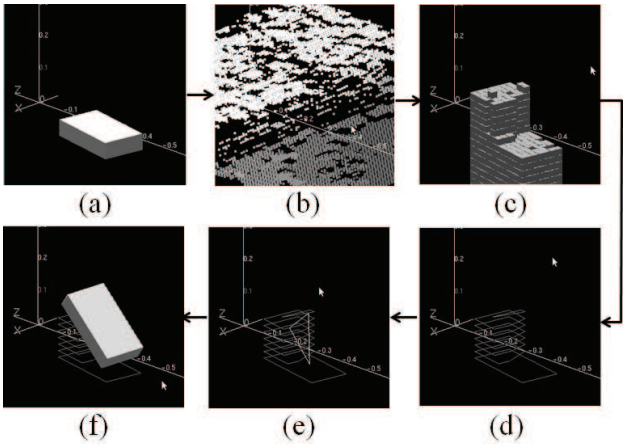

Fig. 5. Landing state estimation algorithm

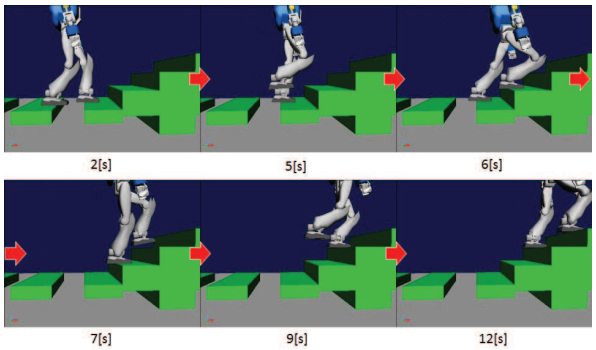

(a) With support region information

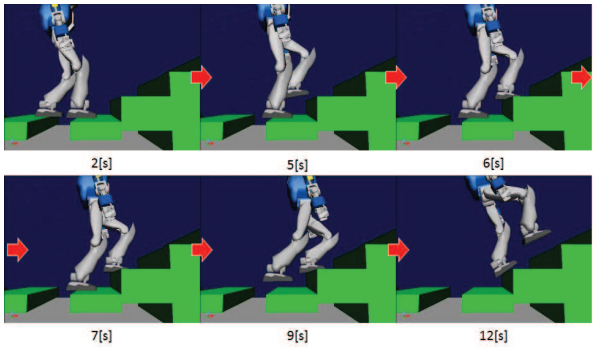

(b) Without support region information

Fig. 6. Uneven walking with/without terrain information

provided in the online pattern generation and the balance control, it will increase the probability of a falling down. In this case, a stable force transition at a double support phase can not be realized because an infeasible torque is requested. Using the support region information, a landing on a narrow space will be permissible. This reduces a burden of the foot planning which searches the feasible landing position. Then a robot can walk around on a more complicated terrain in Fig.7.

In Fig.7, the random height boxs, the discrete flat planes, a few steps stairs, and a pitch and a roll inclination are assigned. The maximum difference height is within 0.15[m]

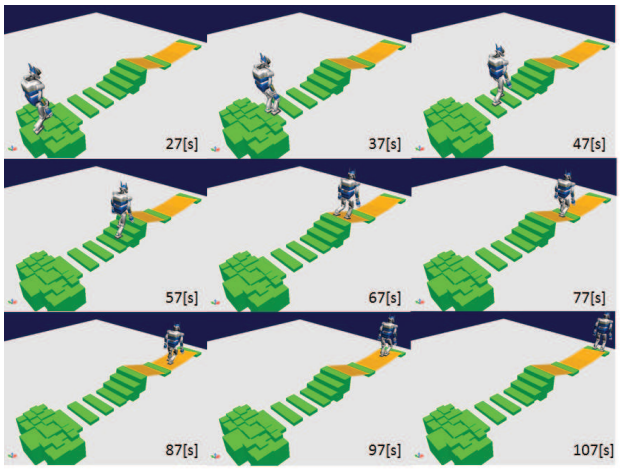

Fig. 7. Complicated uneven walking

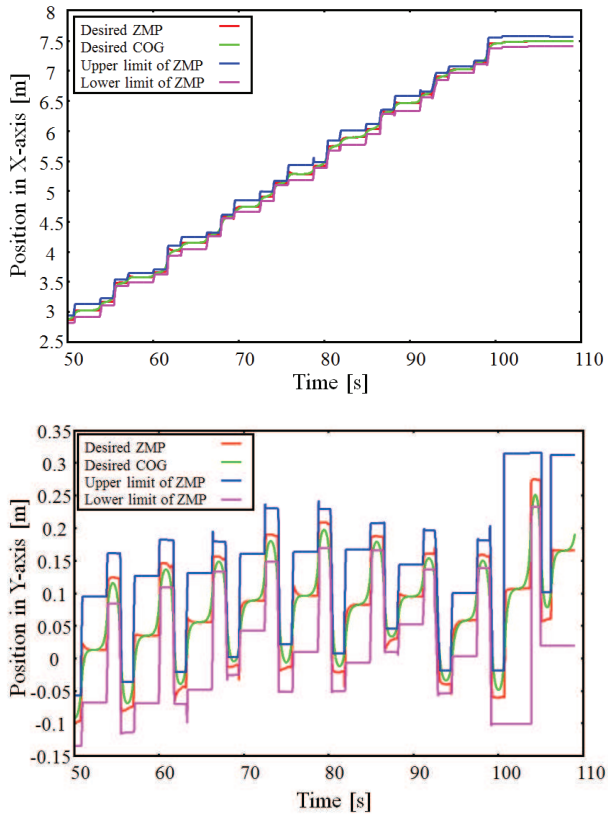

Fig. 8. COG and ZMP trajectories (top:x-axis/bottom:y-axis)

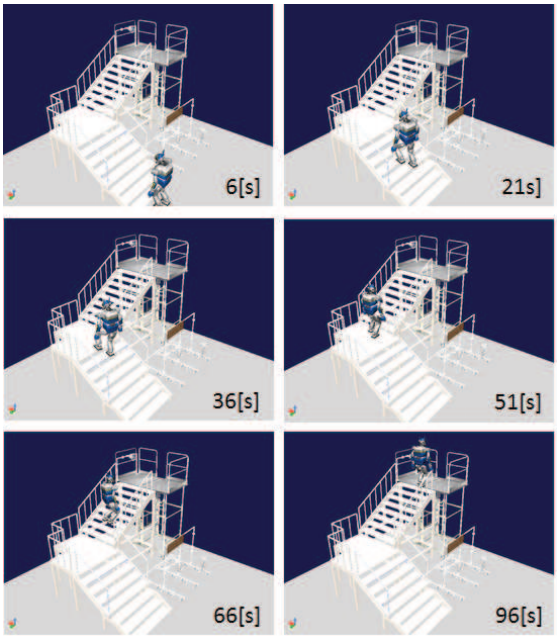

(a) Stair climbing

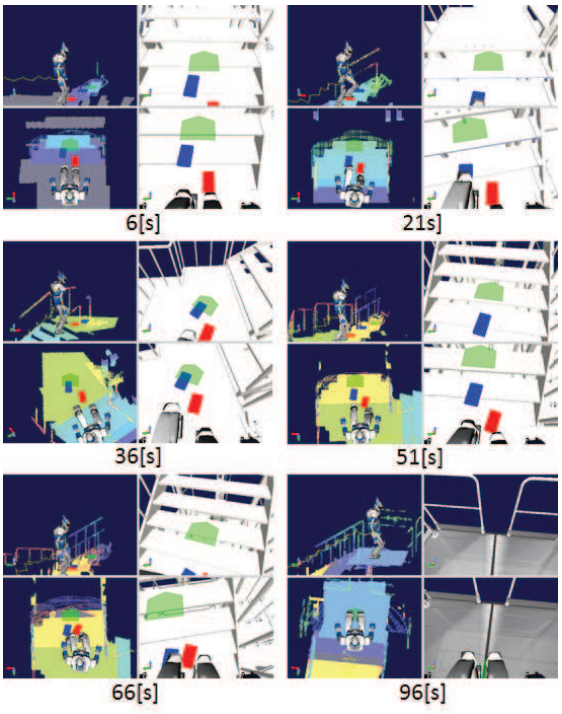

(b) Tele-operation terminal

Fig. 9. Stair climing by tele-operation on Choreonoid

in the environment. The distance of a closest edge between the discrete flat planes is set to 0.3[m]. If the robot tries to land on a full support region, more than 0.5m step length is requested in addition to the foot size. This is relatively hard to travel for our humanoid robot HRP-2 compared with the leg length. The landing state estimation calculates the future landing position and orientation, and the support region at every two steps. The COG and the ZMP trajectories at the last 60 minutes are plotted in Fig.8. The foot size is 0.23x0.13[m] in a forward and a side direction respectively. Therefore, the upper and lower limitation of the ZMP becomes smaller then the foot size during walking, Because the support region is provided spatially as a convex hull, a projection of the ZMP limitation to the time response will be varied. Even at a single support phase, the ZMP limitation is not constant value. The desired ZMP at a single support phase is set to the center of the estimated support region. A overshoot or a undershoot of the ZMP trajectory were appeared by a time adjustment in the pattern generator to a contact on a terrain synchronously.

Walking on more realistic environment are shown in Fig.9 (a). The operator only commands a final goal position to the robot as like in Fig.9 (b). The home base of a pentagon marker as a final goal can be manipulated by a commercial joystick. We prepare four views in the tele-operation terminal. Right two views are actual camera images mounted on a head that are overlaid the final goal marker. Left two views are back-top and side-top bird's eye view with the grid map of the measured terrain and the planned landing steps. Then, an intuitively manipulatable tele-operation terminal for a biped locomotion could be developed.

VI. Conclusion and future work

The new balance control method for a humanoid robot which with a position based joint servo was proposed. The characteristics of the ZMP was modeled as a first order delay system which is taken a characteristics of force controller at inner control loop into account. Information of a support region was utilized to the online pattern generation and a balance controller as a torque limit on the foot, a biped locomotion on complicated terrain with a narrow support region could be realized. Using inverted pendulum model with a first order delay system of the ZMP, the PID controller law of the Capture Point was derived. We also developed tele-operation terminal for a biped locomotion. Walking on a complicated terrain could be achieved by leading a final goal position and direction.

Dealing with a low stiffness or movement terrain, multi contact motion, and experimentation in real environment are our future work to extend a reachable area for a humanoid robot.

VII. ACKNOWLEDGMENTS

This work is partially supported by the NEDO R&D project on disaster-response robots.

References

[1] DARPA Robotics Challenge Trials 2013, http://www.theroboticschallenge.org/content/drc-trials-website-archived

[2] K. Nishiwaki, and S. Kagami, "High Frequency Walking Pattern Generation based on Preview Control of ZMP," *in Proc. of IEEE Int. Conf. on Robotics and Automation*, pp.2667-2672, 2006.

[3] Y. Choi, D. Kim and B-J.You, "On the Walking Control for Humanoid Robot based on the Kinematic Resolution of CoM Jacobian with Embedded Motion,' *in Proc. of IEEE Int. Conf. on Robotics and Automation*, pp.2655-2660, 2006.

[4] P-B. Wieber, "Trajectory free linear model predictive control for stable walking in the presence of strong perturbations," *in Proc. of IEEE-RAS Int. Conf. on Humanoid Robots*, pp.137-142, 2006.

[5] T. Sugihara, "Standing Stabilizability and Stepping Maneuver in Planar Bipedalism based on the Best COM-ZMP Regulator," *in Proc. of IEEE Int. Conf. on Robotics and Automation*, pp.1966-1971, 2009

[6] S. Kajita, M. Morisawa, K. Miura, S. Nakaoka, K. Harada, K. Kaneko, F. Kanehiro, and K. Yokoi, "Biped walking stabilization based on linear inverted pendulum tracking," *in Proc. of IEEE/RSJ Int. Conf. on Intelligent Robots and Systems*, pp.4489-4496, 2010.

[7] J. Pratt, J. Carff, S. Drakunov, and A. Goswami, "Capture Point: A Step toward Humanoid Push Recovery," *in Proc. of IEEE-RAS Int. Conf. on Humanoid Robots*, pp.200-207, 2006.

[8] T. Takenaka, T. Matsumoto, T. Yoshiike, T. Hasegawa, S. Shirokura, H. Kaneko and A. Orita, "Real Time Motion Generation and Control for Biped Robot -4th Report: Integrated Balance Control-," *in Proc. of IEEE/RSJ Int. Conf. on Intelligent Robots and Systems*, pp.1601-1608, 2009.

[9] J. Englsberger, C. Ott, M. A. Roa, A. Albu-Schäffer, and G. Hirzinger, "Bipedal walking control based on Capture Point Dynamics," *in Proc. of IEEE/RSJ Int. Conf. on Intelligent Robots and Systems*, pp.4420-4427, 2011.

[10] J. Englsberger, C. Ott, A. and Albu-Schffer, "Three-dimensional bipedal walking control using Divergent Component of Motion," *in Proc. of IEEE/RSJ Int. Conf. on Intelligent Robots and Systems*, pp.2600-2607, 2013.

[11] M. Morisawa, F. Kanehiro, K. Kaneko, N. Mansard, J. Sola, E. Yoshida, K. Yokoi, and J-P. Laumond, "Combining Suppression of the Disturbance and Reactive Stepping for Recovering Balance," *in Proc. of IEEE Int. Conf. on Intelligent Robots and Systems (IROS)*, pp.3150-3156, 2010.

[12] M. Morisawa, F. Kanehiro, K. Kaneko, S. Kajita, K. Yokoi, "Reactive Biped Walking Control for a Collision of a Swinging Foot on Uneven Terrain," *in Proc. of IEEE-RAS Int. Conf. on Humanoids*, pp.768-773, 2011.

[13] M. Morisawa, et al. "Balance Control based on Capture Point Error Compensation for Biped Walking on Uneven Terrain", *in Proc. of IEEE-RAS Int. Conf. on Humanoids*, pp.734-740, 2012.

[14] K. Nishiwaki, and S. Kagami, "Simultaneous Planning of CoM and ZMP based on the Preview Control Method for Online Walking Control," *in Proc. of IEEE-RAS Int. Conf. on Humanoids*, pp.252-259, 2013.

[15] F. Kanehiro, M. Morisawa, W. Suleiman, K. Kaneko, E. Yoshida, "Integrating geometric constraints into reactive leg motion generation," *in Proc of IEEE/RSK Int. Conf. on Intelligent Robots and Systems* (IROS), pp.4069-4076, 2010.

[16] N. Kita, M. Morisawa, and F. kanehiro, "Foot Landing State Estimation from Point Cloud at a Landing Place," *in Proc. of IEEE-RAS Int. Conf. on Humanoids*, pp.845-851, 2013.

[17] S. Nakaoka, "Choreonoid: Extensible Virtual Robot Environment Built on an Integrated GUI Framework", *in Proc. of the 2012 IEEE/SICE International Symposium on System Integration (SII2012)*, pp.79-85, 2012.